Computational Harmonic Analysis for Tensor Fields on the Two-Sphere

Peter J. Kostelec,* David K. Maslen,* Dennis M. Healy, Jr.,† and Daniel N. Rockmore*,[1]

*Department of Mathematics, Dartmouth College, Hanover, New Hampshire 03755-3551; and †Mathematics
Department, University of Maryland, College Park, Maryland 20742-4015
E-mail: geelong@cs.dartmouth.edu, maslen@cs.dartmouth.edu,
healy@dartmouth.edu, rockmore@cs.dartmouth.edu

In this paper we describe algorithms for the numerical computation of Fourier transforms of tensor fields on the two-sphere, S^2. These algorithms reduce the computation of an expansion on tensor spherical harmonics to expansions in scalar spherical harmonics, and hence can take advantage of recent improvements in the efficiency of computation of scalar spherical harmonic transforms. © 2000 Academic Press

Key Words: harmonic analysis; sphere; tensor fields; Fourier transforms.

1. INTRODUCTION

The calculation of Fourier expansions for vector fields and, more generally, tensor fields on the two-sphere has been identified as an important computational problem in areas such as fluid dynamics [5] and global circulation modeling [18]. Other applications include the analysis of cosmic microwave background radiation [22] and models of stress propagation through the earth [6].

In this paper we show how the computation of expansions in tensor spherical harmonics may be reduced to a small number of scalar spherical harmonic transforms. Over the past 20 years a large body of work has grown, addressing the problem of efficient and stable computation of scalar spherical harmonic transforms [1, 3, 9, 12, 15, 16]. Our reduction of the tensor harmonic transform to scalar harmonic transforms allows this work to be applied to a new set of problems.

Our results generalize a well-known relationship between vector and scalar spherical harmonics (see, e.g., [13]) to the case of tensor spherical harmonics. This relation was used

for analysis of shallow water models by Temperton [19] to reduce the computation of vector harmonics to that of scalar harmonics. Thus, our work can be considered a generalization of Temperton's u-v approach to phenomena that are described by tensor fields.

To verify that our results give a practical method of computing tensor harmonic expansions, we implemented the algorithms and investigated their numerical accuracy experimentally. In the reduction to spherical harmonics some issues of numerical stability do arise, and these are examined. The reduction to spherical harmonic transforms is the main point of this paper, and in the subsequent computation of the transforms, any accurate routine for computing the scalar harmonic transform can be used. For convenience we chose a method based on the so-called "semi-naive" algorithm [2, 9], a technique which computes the necessary discrete Legendre transforms in the frequency domain.

The organization of the paper is as follows. We start in Section 2 with a brief overview of the theory of vector and scalar harmonics. In Section 3 we discuss the tensor spherical harmonics introduced by Newman and Penrose [14] and develop the properties needed to relate these to scalar spherical harmonics. These tensor harmonics are also known as monopole harmonics [20, 21] and are the natural choice for the expansion of tensor fields on the sphere. In Section 4 we develop a sampling theory for tensor fields on the sphere in both the band-limited, and non-band-limited settings. In Section 5 we combine the sampling and tensor harmonic results to get explicit algorithms for computing the expansion of a finitely sampled tensor field in terms of tensor harmonics. We present our numerical results in Section 6 and conclude in Section 7.

2. HARMONIC ANALYSIS ON THE TWO-DIMENSIONAL SPHERE

Since the scalar spherical transform will play a pivotal role in our development of tensor spherical transforms, we first provide a brief review of scalar spherical harmonics. We emphasize their relation to the Laplacian operator and rotation invariance, as these will be the defining properties that we generalize for defining tensor harmonics.

Rotationally invariant differential operators occur throughout the physical sciences. It is a well-known fact that any such operator may be expressed as a sum of powers of the Laplacian, here denoted as Δ. In coordinates, Δ is defined by

$$\Delta = -\left(\frac{\partial^2}{\partial \theta^2} + \cot\theta \frac{\partial}{\partial\theta} + \frac{1}{\sin^2\theta} \frac{\partial^2}{\partial\varphi^2} \right), \tag{1}$$

where θ is the colatitude, and φ is the azimuthal coordinate (cf. Fig. 1).

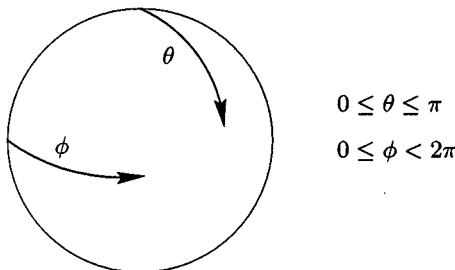$$0 \le \theta \le \pi$$
$$0 \le \phi < 2\pi$$

FIG. 1. Colatitude and azimuthal coordinates.

The spherical harmonics are an orthogonal system of functions on the two-dimensional sphere that diagonalize any rotationally invariant differential operator. This accounts for their ubiquity in problems involving spherical symmetry. In terms of the Laplacian, the spherical harmonics are defined up to a scalar multiple by the properties

$$\Delta Y_{lm} = l(l+1)Y_{lm} \qquad \text{and} \qquad \frac{1}{i}\frac{\partial Y_{lm}}{\partial\varphi} = mY_{lm}. \tag{2}$$

These conditions imply that l and m are integers with $|m| \leq l$.

Mathematicians and physicists use a number of different conventions for the normalization of the spherical harmonics. We normalize things so that the expression for Y_{lm} in coordinates becomes

$$Y_{lm}(\theta, \varphi) = P_{lm}(\cos\theta)e^{im\varphi}, \tag{3}$$

where P_{lm} is the associated Legendre function defined by

$$P_{lm}(x) = \frac{1}{2^l l!}(1 - x^2)^{m/2}\frac{d^{l+m}}{dx^{l+m}}(x^2 - 1)^l. \tag{4}$$

With this normalization, the spherical harmonics satisfy the additional symmetry under complex conjugation, $\overline{Y_{lm}} = Y_{l,-m}$, and have L^2-norm

$$\|Y_{lm}\|_2^2 = \int_0^\pi \int_0^{2\pi} |Y_{lm}(\theta, \varphi)|^2 \sin\theta \, d\varphi \, d\theta = \frac{4\pi}{2l+1} \cdot \frac{(l+m)!}{(l-m)!}. \tag{5}$$

The spherical harmonics are orthogonal with respect to the inner product

$$\langle f, h \rangle = \int_0^\pi \int_0^{2\pi} f(\theta, \varphi)\overline{h(\theta, \varphi)} \sin\theta \, d\varphi \, d\theta. \tag{6}$$

Using this inner product, any square-integrable function on the sphere may be expanded in the spherical harmonic basis. The formula for the expansion is

$$f = \sum_l \sum_{|m| \leq l} \|Y_{lm}\|_2^{-2} \hat{f}(l, m) \cdot Y_{lm}, \tag{7}$$

where the sum converges in the mean, and the coefficients $\hat{f}(l, m)$ are defined by $\hat{f}(l, m) = \langle f, Y_{lm} \rangle$. The function $\hat{f}(l, m)$ is called the *scalar spherical harmonic transform of* f, and as the formulae (3) and (6) for spherical harmonics and inner products show, it may be computed using a Fourier transform on the azimuthal variable φ followed by integration over the colatitude θ.

2.1. *Vector Spherical Harmonics*

So far we have only considered the expansion of a complex scalar function on the sphere in terms of an orthogonal basis of scalar functions, the spherical harmonics. This basis was determined, up to normalization constants, by its properties under rotations of the sphere (cf. (2)) and a choice of a distinguished point (and hence an axis) on the sphere, the north pole.

There is an analogous expansion for vector fields on the sphere. We shall define an inner product on the space of such vector fields and choose a basis for the resulting Hilbert space, the *vector spherical harmonics*, based on a set of specified properties under rotation, and in this way generalize the construction of the scalar spherical harmonics. Consequently, in the same way that scalar spherical harmonics are used in spectral method approaches for numerical solution of scalar PDEs or data analysis of scalar data on the sphere, the vector spherical harmonics may be used effectively in cases where the data consist of vector fields on the sphere. Typical examples that arise in practice are electromagnetic fields or wind velocity.

We start our analysis by noting that we need only consider tangential vector fields on the sphere. If we consider the sphere as embedded in 3-space, then it is natural to view any vector field as the direct sum of a purely radial field and an orthogonal tangential field. The purely radial vector fields transform under rotations in exactly the same way as scalar fields, and so the appropriate basis for the subspace of purely radial vector fields consists of the fields of the form $Y_{lm}\mathbf{e}_r$, where $\mathbf{e}_r$ is the radial vector field of unit vectors. Hence, radial vector fields may be treated using the methods developed for scalar spherical harmonics. The complementary space of vector fields, the tangential vector fields, requires a separate treatment.

Any tangential vector field on the sphere can be expressed, except at the poles, in terms of the usual unit vector fields $\mathbf{e}_\theta$ and $\mathbf{e}_\varphi$ which are generated by polar coordinates (θ, φ) [18]. I.e., any real tangential vector field $\mathbf{v}$ may be written as

$$\mathbf{v} = v_\theta \mathbf{e}_\theta + v_\varphi \mathbf{e}_\varphi,$$

where v_θ and v_φ are real-valued functions defined on S^2 except at the poles. For our purposes it is most convenient, though not essential, to work with complex vector fields, in which case the functions v_θ and v_φ are complex-valued. Given two tangential vector fields, $\mathbf{u}$ and $\mathbf{v}$, define their inner product to be

$$\langle \mathbf{u}, \mathbf{v} \rangle = \int_{S^2} u_\theta \overline{v_\theta} + u_\varphi \overline{v_\varphi} \, d\mu, \tag{8}$$

where $d\mu = \sin \theta \, d\theta \, d\varphi$ is the invariant measure on the sphere; we denote the corresponding Hilbert space by $L^2_T(S^2)$.

In order to generalize the eigenvalue equations (2), we must generalize the Laplacian and angular momentum operators to act on tangential vector fields. The Laplacian of the vector field $\mathbf{v} = v_\theta \mathbf{e}_\theta + v_\varphi \mathbf{e}_\varphi$ can be defined using the Riemannian metric on the sphere or as the image of the Casimir operator under the action of the rotation group. In either case, the formula in coordinates is

$$\Delta \mathbf{v} = \left[-\left(\frac{\partial^2}{\partial \theta^2} + \cot \theta \frac{\partial}{\partial \theta} + \frac{1}{\sin^2 \theta} \frac{\partial^2}{\partial \varphi^2} - \frac{1}{\sin^2 \theta} \right) v_\theta + \frac{2 \cot \theta}{\sin \theta} \frac{\partial v_\varphi}{\partial \varphi} \right] \mathbf{e}_\theta$$
$$+ \left[-\left(\frac{\partial^2}{\partial \theta^2} + \cot \theta \frac{\partial}{\partial \theta} + \frac{1}{\sin^2 \theta} \frac{\partial^2}{\partial \varphi^2} - \frac{1}{\sin^2 \theta} \right) v_\varphi - \frac{2 \cot \theta}{\sin \theta} \frac{\partial v_\theta}{\partial \varphi} \right] \mathbf{e}_\varphi. \tag{9}$$

The angular momentum operator is defined by

$$J_z \mathbf{v} = \frac{1}{i} \frac{\partial v_\theta}{\partial \varphi} \mathbf{e}_\theta + \frac{1}{i} \frac{\partial v_\varphi}{\partial \varphi} \mathbf{e}_\varphi \tag{10}$$

and is the infinitesimal generator for rotations around the z-axis.

The vector spherical harmonics, $\mathbf{B}_{lm}$ and $\mathbf{C}_{lm}$, are defined so that they satisfy the differential equations

$$\Delta\mathbf{A}_{lm} = l(l+1)\mathbf{A}_{lm} \tag{11}$$

and

$$J_z\mathbf{A}_{lm} = m\mathbf{A}_{lm}. \tag{12}$$

The conditions (11) and (12) are analogous to the conditions (2) for the scalar spherical harmonics, but unlike the scalar case, these equations have a two-dimensional space of solutions for each l and m with $l \geq 1$ and $|m| \leq l$, giving rise to two independent vector spherical harmonics, $\mathbf{B}_{lm}$ and $\mathbf{C}_{lm}$.

Following Morse and Feshbach [13], if we define

$$\mathbf{B}_{lm} = \frac{1}{\sqrt{l(l+1)}}\left[\frac{\partial Y_{lm}}{\partial\theta}\mathbf{e}_\theta + \frac{1}{\sin\theta}\frac{\partial Y_{lm}}{\partial\varphi}\mathbf{e}_\varphi\right]$$

and

$$\mathbf{C}_{lm} = -\mathbf{e_r} \times \mathbf{B}_{lm}$$

then $\mathbf{B}_{lm}$ and $\mathbf{C}_{lm}$ each satisfy the eigenvalue equations (11) and (12). The collection of vector fields $\{\mathbf{B}_{lm}, \mathbf{C}_{lm}\}$ for $1 \leq l$ and $|m| \leq l$ forms a complete basis of orthogonal vector fields in the space of all tangential vector fields, with normalization constants the same as for the scalar spherical harmonics, i.e.,

$$\|\mathbf{B}_{lm}\|^2 = \|\mathbf{C}_{lm}\|^2 = \|Y_{lm}\|^2 = \frac{4\pi}{2l+1}\frac{(l+m)!}{(l-m)!}.$$

Hence any vector field on the sphere may be written as

$$\mathbf{v} = \sum_{1\leq l, |m|\leq l}\frac{1}{\|Y_{lm}\|^2}[f^B(l,m)\mathbf{B}_{lm} + f^C(l,m)\mathbf{C}_{lm}],$$

where $f^B(l,m) = \langle\mathbf{v}, \mathbf{B}_{lm}\rangle$ and $f^C(l,m) = \langle\mathbf{v}, \mathbf{C}_{lm}\rangle$. The map from the vector field $\mathbf{v}$ to the coefficients $\{f^B(l,m), f^C(l,m)\}$ is called the *vector harmonic transform*.

To relate the vector harmonic transform to the scalar harmonic transform, simply note that

$$\mathbf{B}_{lm} = \frac{1}{\sqrt{l(l+1)}}\frac{1}{\sin\theta}\left[\frac{1}{2l+1}[l(l-m+1)Y_{l+1,m} - (l+1)(l+m)Y_{l-1,m}]\mathbf{e}_\theta + imY_{lm}\mathbf{e}_\varphi\right]$$

and

$$\mathbf{C}_{lm} = \frac{1}{\sqrt{l(l+1)}}\frac{1}{\sin\theta}\left[imY_{lm}\mathbf{e}_\theta - \frac{1}{2l+1}[l(l-m+1)Y_{l+1,m} - (l+1)(l+m)Y_{l-1,m}]\mathbf{e}_\varphi\right].$$

Hence, if we define auxiliary quantities $g^\theta(l, m)$ and $g^\varphi(l, m)$ by

$$g^\theta(l, m) = \left\langle \frac{1}{\sin\theta} v_\theta, Y_{lm} \right\rangle, \tag{13}$$

$$g^\varphi(l, m) = \left\langle \frac{1}{\sin\theta} v_\varphi, Y_{lm} \right\rangle \tag{14}$$

then

$$f^B(l, m) = \frac{1}{\sqrt{l(l+1)}} \left[\frac{l(l-m+1)}{2l+1} g^\theta(l+1, m) \right.$$
$$\left. - \frac{(l+1)(l+m)}{2l+1} g^\theta(l-1, m) - img^\varphi(l, m) \right] \tag{15}$$

$$f^C(l, m) = \frac{1}{\sqrt{l(l+1)}} \left[-img^\theta(l, m) - \frac{l(l-m+1)}{2l+1} g^\varphi(l+1, m) \right.$$
$$\left. + \frac{(l+1)(l+m)}{2l+1} g^\varphi(l-1, m) \right]. \tag{16}$$

Equations (15) and (16) allow us to compute a vector harmonic transform by means of two scalar transforms. Once we have calculated the quantities $g^\theta(l, m)$ and $g^\varphi(l, m)$ for $l \geq 1$ and $|m| \leq l \leq N+1$ (this will be discussed in Section 3), we may use Eqs. (15) and (16) to calculate $f^B(l, m)$ and $f^C(l, m)$ for $1, |m| \leq l \leq N$ in an additional $6((N+1)^2 - 1)$ scalar multiplications and $4((N+1)^2 - 1)$ scalar additions.

3. HARMONIC ANALYSIS OF TENSOR FIELDS

3.1. *The Spin-s Harmonics*

There are several different definitions of tensor spherical harmonics which have been developed in the study of quantum mechanical angular momentum, gravitational radiation and group representations. The spin-s harmonics are an orthogonal basis of tensor fields that seems particularly well suited to the harmonic analysis of tensor fields, of any rank, on the sphere. These tensor fields were introduced by Gel'fand, Minlos, and Shapiro [7] and were rediscovered by Newman and Penrose [14] who named them spin-s harmonics. Wu and Yang [20, 21] later defined equivalent versions of these tensor harmonics, calling them monopole harmonics. Our exposition follows the construction used in [8, 14].

The first step in our construction is to introduce a set of basis vectors and tensors at each point of the sphere apart from the poles. The fields $\mathbf{e}_\theta$ and $\mathbf{e}_\varphi$ are easily visualized, but are not the most convenient fields to work with, because fields of the form $v_\theta \mathbf{e}_\theta$ or $v_\varphi \mathbf{e}_\varphi$ are not transformed onto fields of the same type under rotations. Define the fields $\mathbf{e}_+$ and $\mathbf{e}_-$ by

$$\mathbf{e}_+ = \frac{1}{\sqrt{2}} (\mathbf{e}_\theta - i\mathbf{e}_\varphi), \qquad \mathbf{e}_- = \frac{1}{\sqrt{2}} (\mathbf{e}_\theta + i\mathbf{e}_\varphi).$$

As with the fields $\mathbf{e}_\theta$, $\mathbf{e}_\varphi$, the vectors $\mathbf{e}_+$, $\mathbf{e}_-$ are orthonormal at each point of the sphere apart from the north and south poles. However, the set of fields of the form $v_\pm \mathbf{e}_\pm$ is invariant under rotations and is also much better behaved at the poles; the lines generated by the vectors $\mathbf{e}_\pm$ converge to unique lines at each pole. I.e., the fields $\mathbf{e}_\pm$ are sections of homogeneous

subbundles of the tangent bundle, away from the poles. Given a tangent vector field $\mathbf{v}$, we may write $\mathbf{v} = v_+\mathbf{e}_+ + v_-\mathbf{e}_-$, where $v_\pm = \frac{1}{\sqrt{2}}(v_\theta \pm i v_\varphi)$. In this notation the inner product (8) can be rewritten as

$$\langle \mathbf{u}, \mathbf{v} \rangle = \int_{S^2} u_+\overline{v_+} + u_-\overline{v_-}\, d\mu.$$

We denote the set of vector fields of the form $v_\pm\mathbf{e}_\pm$, by $L^2(E_{\pm 1})$.

Now construct fields of basis tensors generalizing $\mathbf{e}_+$ and $\mathbf{e}_-$. Let $\mathbf{e}_0 = 1$, and for $n \geq 1$ define

$$\mathbf{e}_n = \mathbf{e}_+ \otimes \cdots \otimes \mathbf{e}_+, \qquad \mathbf{e}_{-n} = \mathbf{e}_- \otimes \cdots \otimes \mathbf{e}_-,$$

where the tensor products $\mathbf{e}_{\pm n}$ have n factors. There is a natural identification $\mathbf{e}_n \otimes \mathbf{e}_m = \mathbf{e}_{n+m}$ for any integers n, m, and we can use this identification to reduce the problem of finding harmonic expansions of arbitrary tensor fields on the sphere to the problem of expanding fields of the form $f\mathbf{e}_n$. A tensor field of the form $f\mathbf{e}_n$ is called a *tensor field of type n or a tensor field with spin weight n* [14]. Let $L^2(E_n)$ denote the vector space of square integrable tensor fields of type n, with the inner product

$$\langle f\mathbf{e}_n, g\mathbf{e}_n \rangle = \int_{S^2} f\bar{g}\, d\mu.$$

The definition of the tensor spherical harmonics is formally identical to the scalar harmonics, except that the Laplacian and angular momentum operators occurring in (2) are defined for tensor fields of type n instead of scalar fields. In coordinates, the Laplacian and angular momentum operators on tensor fields of type n are given by

$$\Delta(f\mathbf{e}_n) = -\left[\left(\frac{\partial^2}{\partial\theta^2} + \cot\theta\,\frac{\partial}{\partial\theta} + \frac{1}{\sin^2\theta}\frac{\partial^2}{\partial\varphi^2} + \frac{2ni\cot\theta}{\sin\theta}\frac{\partial}{\partial\varphi} - \frac{n^2}{\sin^2\theta}\right)f\right]\mathbf{e}_n$$

and

$$J_z(f\mathbf{e}_n) = \left[\frac{1}{i}\frac{\partial}{\partial\varphi}f\right]\mathbf{e}_n.$$

Then any invariant differential operator, from tensor fields of type n to tensor fields of type n, is a sum of powers of the Laplacian, and the spin-n harmonics are defined up to a scalar multiple as solutions to the eigenvalue equations

$$\Delta\mathbf{Y}_{lm}^n = l(l+1)\mathbf{Y}_{lm}^n \qquad \text{and} \qquad J_z\mathbf{Y}_{lm}^n = m\mathbf{Y}_{lm}^n. \tag{17}$$

To construct explicit formulae for the spin-n harmonics, we use invariant differential operators between spaces of smooth tensor fields of different types. Define differential operators $D_\pm$ from smooth tensor fields of type n to smooth tensor fields of type $n \pm 1$ by

$$D_\pm(f\mathbf{e}_n) = \left[\left(\frac{\partial}{\partial\theta} \pm \frac{i}{\sin\theta}\frac{\partial}{\partial\varphi} \mp n\cot\theta\right)f\right]\mathbf{e}_{n\pm 1}. \tag{18}$$

Newman and Penrose [14] use the notation $\eth$ for D_+ and $\bar{\eth}$ for D_-. We also define operators $D_{\pm n}$ to be $D_\pm \cdots D_\pm$ (n factors) for $n > 0$.

Remark. Equation (18) defines differential operators acting on sections away from the north and south pole, but the differential operators extend smoothly to the entire sphere. This can be seen by looking at the action of $SO(2)$ on the universal enveloping algebra of $so(3)$. For any p, n, the space of differential operators from tensor fields of type n to tensor fields of type $n + p$ is generated by D_p both as a left module over the invariant differential operators on tensors of type $n + p$ and as a right module over the invariant differential operators on tensors of type n. A second way of constructing these generators is to project the covariant derivative onto subbundles of the tensor bundles of S^2.

Let

$$C_{nl} = \prod_{k=0}^{|n|-1} (l(l+1) - k(k+1)).$$

Then, the operators $D_\pm$, $D_{\pm n}$ satisfy the following properties:

LEMMA 3.1.

    (i) $D_\pm$ *are rotationally invariant differential operators.*
    (ii) $D_\pm \Delta = \Delta D_\pm$ *and* $J_z D_\pm = D_\pm J_z$.
    (iii) $D_\pm^* = -D_\mp = -\overline{D_\pm}$.
    (iv) $D_+^* D_+ = \Delta - n(n+1)$ *and* $D_+ D_+^* = \Delta - (n-1)n$.
    (v) $\|D_n Y_{lm}\|^2 = C_{nl} \cdot \|Y_{lm}\|^2$.

DEFINITION 3.1.   Define the monopole harmonics of type n, degree l, and order m to be

$$\mathbf{Y}_{lm}^n = \frac{1}{\sqrt{C_{nl}}} D_n Y_{lm} \mathbf{e}_0. \tag{19}$$

We shall also call these the tensor spherical harmonics.

Equations (17) and (19) now imply that the functions $\mathbf{Y}_{lm}^n$ make up a basis for $L^2(E_n)$.

THEOREM 3.1.   *The set of functions* $\{\mathbf{Y}_{lm}^n : |n| \leq l, |m| \leq l\}$, *defined in* (19), *is an orthogonal basis for* $L^2(E_n)$, *satisfying* (17), *and such that* $\|\mathbf{Y}_{lm}^n\|^2 = \|Y_{lm}\|^2$. *Any such basis for* $L^2(E_n)$ *is uniquely determined up to phase factors.*

Thus, by Theorem 3.1 any tensor field, $\mathbf{v} = f\mathbf{e}_n$, of type n has an expansion

$$\mathbf{v} = \sum_{|n|,|m| \leq l} \frac{1}{\|Y_{lm}\|^2} f_{lm}^n \mathbf{Y}_{lm}^n,$$

where

$$f_{lm}^n = \langle \mathbf{v}, \mathbf{Y}_{lm}^n \rangle = \int_{S^2} f \cdot \overline{X_{lm}^n} \, d\mu$$

and X_{lm}^n is a function on S^2 such that $\mathbf{Y}_{lm}^n = X_{lm}^n \mathbf{e}_n$. The function $f^n(l, m)$ is called the *tensor harmonic transform of the tensor field f.*

EXAMPLE 3.1.   The spin-1 and spin-(-1) harmonics are simply related to the vector spherical harmonics of [13] through the equations

$$\mathbf{B}_{lm} = \frac{1}{\sqrt{2}}\left[\mathbf{Y}_{lm}^{+1} + i\mathbf{Y}_{lm}^{-1}\right]$$

$$\mathbf{C}_{lm} = -\frac{1}{\sqrt{2}}\left[i\mathbf{Y}_{lm}^{+1} + \mathbf{Y}_{lm}^{-1}\right].$$

The fields $\mathbf{B}_{lm}$, $\mathbf{C}_{lm}$ have the advantage of being real, at a cost of poorer invariance properties.

Just as in the case of vector spherical harmonics, our definition of the tensor harmonics (Definition 3.1) is given in terms of derivatives of the scalar spherical harmonics, but for computational purposes we may require a more explicit definition in terms of linear combinations of products of trigonometric functions and scalar harmonics, i.e., we would like an expression for the X_{lm}^n. To this end, define the differential operator

$$B = \frac{\partial}{\partial\theta} + \frac{i}{\sin\theta}\frac{\partial}{\partial\varphi}, \tag{20}$$

and let $B_0 = B$, and then for $n \geq 0$, define

$$B_n = (B - (n-1)\cot\theta)\cdots(B - \cot\theta)B$$

and $B_{-n} = \overline{B_n}$. From this we see that

$$X_{lm}^n = \frac{1}{\sqrt{C_{nl}}}B_n Y_{lm}.$$

LEMMA 3.2.   *With B defined as in (20),*

$$(B - n\cot\theta)\frac{1}{(\sin\theta)^k}Y_{lm} = \frac{1}{(\sin\theta)^{k+1}}\frac{1}{2l+1}[(l-m+1)(l-n-k)Y_{l+1,m}$$
$$- (l+m)(l+1+n+k)Y_{l-1,m} - (2l+1)mY_{lm}]$$

and

$$(\bar{B} + n\cot\theta)\frac{1}{(\sin\theta)^k}Y_{lm} = \frac{1}{(\sin\theta)^{k+1}}\frac{1}{2l+1}[(l-m+1)(l+n-k)Y_{l+1,m}$$
$$- (l+m)(l+1-n+k)Y_{l-1,m} + (2l+1)mY_{lm}].$$

Consequently, we can now define the X_{lm}^n directly in terms of the scalar spherical harmonics.

COROLLARY 3.1.   *There are constants $c_{l,p,m}^n$ such that*

$$X_{lm}^n = \sum_{p=l-n}^{l+n} c_{l,p,m}^n \frac{1}{(\sin\theta)^{|n|}}Y_{p,m},$$

where the $c^n_{l,p,m}$ satisfy $c^0_{l,l,m} = 1$, $c^0_{l,p,m} = 0$ for $p \neq l$, $c^{-n}_{l,p,m} = c^n_{l,p,-m}$, and the recurrence relation

$$c^{n+1}_{l,p,m} = \frac{1}{\sqrt{l(l+1) - n(n+1)}} \left[-mc^n_{l,p,m} + \frac{(p-m)(p-2n-1)}{2p-1} c^n_{l,p-1,m} \right.$$
$$\left. + \frac{-(p+m+1)(p+2+2n)}{2p+3} c^n_{l,p+1,m} \right]$$

for $l - n \leq p \leq l + n$, $n \leq l$, and $c^n_{l,p,m} = 0$ for $p < l - n$ or $p > l + n$.

Proof. The first two properties of the $c^n_{l,p,m}$ are obvious. The third comes from the equation $X^{-n}_{l,m} = \overline{X^n_{l,-m}}$ (which follows from the fact that $\overline{Y_{lm}} = Y_{l,-m}$, and hence $\overline{\mathbf{Y}^n_{lm}} = \mathbf{Y}^{-n}_{l,-m}$). The recurrence relation comes from the identities of the previous lemma and the relation

$$X^{n+1}_{lm} = \frac{1}{\sqrt{l(l+1) - n(n+1)}} (B - n \cot \theta) X^n_{lm}.$$

∎

In Fig. 2 we plot $X^n_{lm}(\theta, 0)$ for various values of m and l. As we might expect from their definition, their graphs are very similar to that of associated Legendre functions.

Using Corollary 3.1 we can now give an algorithm for calculating the tensor spherical transform of type n for $|n| \leq l \leq N$ using a single scalar spherical transform which we need only compute for all orders l, with $0 \leq l \leq N + |n|$. Starting with a tensor field, $f\mathbf{e}_n$, we compute the auxiliary quantities

$$g^n(l, m) = \left\langle \frac{1}{(\sin \theta)^{|n|}} f, Y_{lm} \right\rangle \tag{21}$$

for $0 \leq l \leq N + |n|$ using a scalar spherical transform. We then use the relations

$$f^n(l, m) = \sum_{p=l-n}^{l+n} \overline{c^n_{l,p,m}} g^n(p, m) \tag{22}$$

to calculate the tensor harmonic transform in an additional $(2n + 1)[(N + 1)^2 - n^2]$ scalar multiplications and $2n[(N + 1)^2 - n^2]$ scalar additions.

Numerically speaking, the expansion of the X^n_{lm}s given in Corollary 3.1 may give one pause. The X^n_{lm}s are expanded in terms of singular functions, some of which are not even in L^2. (This "pause" is warranted, as will be seen during our discussion of numerical results in Section 6.) What does this result in? Bad condition numbers, unfortunately. For example, in Eq. (21), if $f = 1$ and $|n| > 1$, then $g^n(0, 0) = \infty$. This infinity must cancel with another infinity to give the correct coefficient, which is of order one. The constant function is not band-limited in this context, but for its projection onto the band-limit B (via sampling) we should have $g^n(0, 0) = O(B^{|n|-2})$ or so for $|n| > 2$. There are two alternative approaches that may work for larger n. First, if X^n_{lm} has a recurrence in l, the techniques in [3, 9] can be used. Second, if X^n_{lm} has a nice oscillation structure in θ, the techniques in [12] can be used.
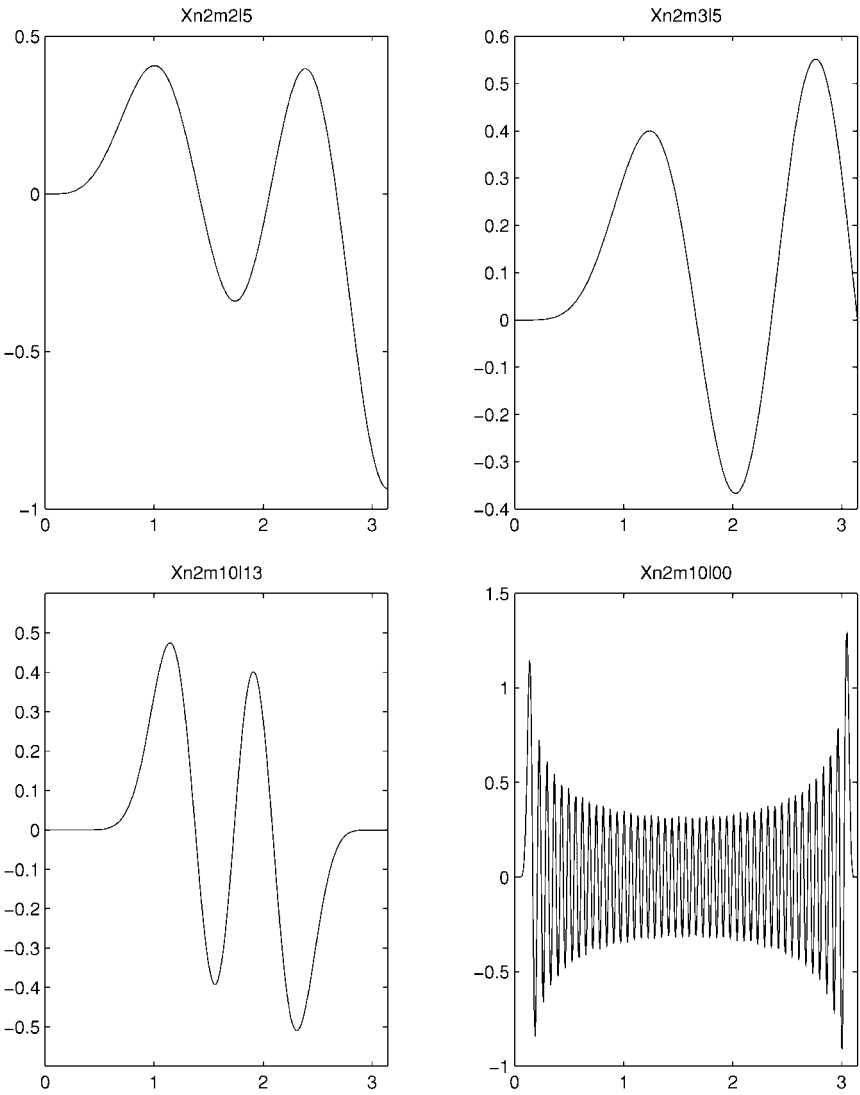
FIG. 2. Plot of $X_{lm}^2(\theta, 0)$ for various values of l and m as a function of θ, at bandwidth 255: top left: $m = 2$, $l = 5$; top right: $m = 3$, $l = 5$; lower left: $m = 10$, $l = 13$; lower right: $m = 10$, $l = 100$.

4. SAMPLING THEOREMS

In order to compute spherical harmonic transforms numerically, we must reduce them, at least approximately, to a finite problem. This means restricting ourselves to a finite number of Fourier coefficients and representing functions by their values at a finite number of points. The simplest sampling theory is the band-limited theory, which explains how to reconstruct a polynomial on the sphere from its values at a finite number of points.

DEFINITION 4.1. A tensor field $f\mathbf{e}_n$ of type n on S^2 is band-limited with band-limit B, if $f^n(l, m) = 0$ for all $l > B$. The space of such tensor fields is denoted $\mathcal{F}_B(E_n)$, so that

$$\mathcal{F}_B(E_n) = \operatorname{span}_{\mathbf{C}}\left\{\mathbf{Y}_{lm}^n : |n|, |m| \le l \le B\right\}.$$

Let $\mathcal{F}(E_n)$ be the union of $\mathcal{F}_B(E_n)$ for all $B > 0$. In the case $n = 0$ we write $\mathcal{F}_B(E_0) = \mathcal{F}_B = \mathcal{F}_B(S^2)$ and $\mathcal{F} = \mathcal{F}(E_0)$.

The most important property of spaces of band-limited tensors is that the product of a tensor field of band-limit B_1 with a tensor field of band-limit B_2 has band-limit $B_1 + B_2$. I.e.,

LEMMA 4.1.

(i) $\mathcal{F}_{B_1}(E_{n_1}) \otimes \mathcal{F}_{B_2}(E_{n_2}) \subseteq \mathcal{F}_{B_1+B_2}(E_{n_1+n_2})$.
(ii) $\mathcal{F}_{B_1} \cdot \mathcal{F}_{B_2}(E_n) \subseteq \mathcal{F}_{B_1+B_2}$.

Given a complex measure s on S^2, we define the *Fourier transform* of s to be the function

$$\hat{s}(l, m) = \int_{S^2} \overline{Y_{lm}} \, ds.$$

If $\mathbf{T} = f\mathbf{e}_n$ is a continuous tensor field of type n on S^2, then we may form the product $s.\mathbf{T}$, and the spherical transform of this product is the function

$$\widehat{s.\mathbf{T}}(l, m) = \int_{S^2} f.\overline{X_{lm}^n} \, ds.$$

When the tensor field is band-limited, there are simple conditions on the measure s, to ensure agreement of the low degree Fourier coefficients of $\mathbf{T}$ and $s.\mathbf{T}$, defined as $\{\hat{\mathbf{T}}(l, m)\}$ and $\{\widehat{s.\mathbf{T}}(l, m)\}$, respectively.

THEOREM 4.1 (Band-limited sampling).   *Assume that s is a complex measure on S^2 such that $\hat{s}(l, m) = \delta_{0,l}$ for $|m| \le l \le 2B$ and $\mathbf{T}$ is band-limited of band-limit B. Then $\widehat{s.T}(l, m) = \hat{T}(l, m)$ for $|m| \le l \le B$.*

Proof.   The condition on s implies that as linear functionals, s and the invariant measure μ agree on the space $\mathcal{F}_{2B}$. Assume, then, that this condition holds and that $\mathbf{T}$ is in $\mathcal{F}_B(E_n)$ and $l \le B$. Then $Y_{l,-m}^{-n}$ is in $\mathcal{F}_B(E_{-n})$, and by the lemma, $\mathbf{T} \otimes Y_{l,-m}^{-n}$ is in $\mathcal{F}_{2B}$. But $\widehat{s.\mathbf{T}}(l, m) = s(\mathbf{T} \otimes Y_{l,-m}^{-n})$.   ∎

The measure s appearing in Theorem 4.1 shall be called *the sampling measure*.

The most commonly used sampling measures have support on either an equiangular grid or a Gaussian grid. For the algorithms discussed in the following sections, we shall use an equiangular grid, although a Gaussian grid (with points equally spaced in the φ direction, and $\cos^{-1}(\theta)$ a root of a Legendre polynomial) is also possible. The following is a slight variation of the sampling theorem given in [3]. Sampling at the north pole and slightly different normalizing of the Legendre polynomials completely account for the differences between the expression for the weights a_j and those given there [3, p. 216].

LEMMA 4.2.   *Let $s = \frac{\sqrt{2\pi}}{2B} \sum_{j=0}^{2B-1} \sum_{i=0}^{2B-1} a_j^{(B)} \delta_{(\theta_j, \varphi_k)}$ where the sample points are chosen from the usual equiangular grid, $\theta_j = \pi(2j+1)/4B$, $\varphi_k = 2\pi k/2B$, and the weights a_j have a closed form expression*

$$a_j = \frac{2}{B} \sin\left(\frac{\pi(2j+1)}{4B}\right) \sum_{k=0}^{B-1} \frac{1}{2k+1} \sin\left((2j+1)(2k+1)\frac{\pi}{4B}\right). \tag{23}$$

Then $\hat{s}(l, m) = 0$ for $|m| \le l \le 2B - 1$.

In the case that the tensor field is not band-limited, Lemma 4.3 shows that via sampling we may still obtain an approximation to its Fourier coefficients.

LEMMA 4.3.   *Assume s is a measure on S^2 such that $\hat{s}(l, m) = \delta_{0,l}$ for $|m| \le l \le 2B$. Assume that $\mathbf{T}$ is a continuous tensor field of type n, and let $\mathbf{S} = s.\mathbf{T}$. Then,*

$$\sum_{l=|n|}^{B} (2l+1) \left[\sum_{|m| \le l} (\hat{\mathbf{T}}(l, m) - \hat{\mathbf{S}}(l, m))^2 \right]^{1/2}$$

$$\le (B+1)^2 (1 + 4B + B^2) \|s\|_1 \sum_{B+1, |n| \le l} (2l+1) \left[\sum_{|m| \le l} \hat{\mathbf{T}}(l, m)^2 \right]^{1/2},$$

where $\|s\|_1$ is the total variation norm of s.

For a proof of this result see [11] or [10].

5. COMPUTATIONAL HARMONIC ANALYSIS

Assume s is a finitely supported measure on the sphere, $\mathbf{T}$ is a continuous tensor field of type n, and B is a positive integer. We now consider the problem of computing the Fourier coefficients $\widehat{s.\mathbf{T}}(l, m)$ for $|n|, |m| \le l \le B$, given the values of $\mathbf{T}$ at the support of s. To see that this amounts to the computation of some finite sums, let S be the support of s, and for each point p in S, let w_p be the weight associated with that point. S is called the *sampling set*. Thus

$$s = \sum_{p \in S} w_p \delta_p.$$

Then, if $T = f.\mathbf{e}_n,$[2] we have

$$\widehat{s.\mathbf{T}}^n(l, m) = \sum_{p \in S} w_p f(p) \overline{X_{lm}^n}.$$

The method we propose for this calculation reduces the problem to a number of simpler transforms.

The first reduction is to express the transforms for vector or tensor harmonics in terms of scalar spherical harmonic transforms. We have already seen that the transform for a type n tensor field may be written in terms of a single larger transform for complex functions.

Having done this reduction, the scalar spherical harmonic transform may be performed using any of a variety of algorithms, e.g., see [1–4, 9, 12, 15, 16].

5.1. *Vector and Tensor Sphericals*

Once we have a method of computing a spherical harmonic transform, the vector and tensor harmonic transforms are easy. For the vector case, Eqs. (13)–(16) define how to

---

[2] If S contains either the north or the south pole, then we are forced to make a choice for the value of $\mathbf{e}_n$ at the poles. The definition of f at the poles will then reflect that choice, and f will have a discontinuity there to match that of $\mathbf{e}_n$.

express vector spherical coefficients in terms of scalar coefficients. For the tensor case, Eqs. (21) and (22) are the critical ones.

The only thing which might give the reader pause is the computation of the "extra" scalar coefficients that are required to determine the highest degree vector and tensor coefficients. As is stated at the end of Section 3.1, the first step in calculating a tensor spherical transform of type n with band-limit B is to compute

$$g^n(l, m) = \left\langle \frac{1}{(\sin \theta)^{|n|}} f, Y_{lm} \right\rangle$$

for $0 \leq l \leq B + |n|$ using a scalar spherical transform. For nonzero n, the computation of $g^n(l, m)$ involves scalar spherical coefficients with degrees greater than the band-limit. Therefore we are projecting signals onto associated Legendre functions with degrees greater than the band-limit. The reason the final result makes sense is that the sampling theory needed to justify the computation only applies to the tensor fields $f \mathbf{e}_n$. We do not need any sampling results to justify the validity of the scalar harmonic transforms in the intermediate stages of our computation.

6. NUMERICAL RESULTS

In this section we present results that indicate that a tensor spherical transform of type n can be performed in a stable fashion for a useful range of problem sizes (i.e., band-limits B) and ranks. For a detailed discussion of the stability and efficiency of several (non-multipole-based) scalar spherical transform algorithms, we refer the reader to [9].

Experiments were performed on a DEC Alpha 500/200 and a SGI Origin 2000, and all code used was based on SpharmonicKit [17]. As noted in Section 2, the scalar spherical transform of a function $f(\theta, \varphi)$ is equivalent to a Fourier transform on the azimuthal angle ϕ followed by an associated Legendre transform on the colatitude angle θ. To perform the scalar spherical transform, we used the semi-naive algorithm (as it is referred to in [9]). Originally developed by Dilts [2], this algorithm can compute the spherical transform of a function f in no more than $O(B^3)$ operations. The Dilts algorithm takes advantage of the fact that the cosine expansion of an associated Legendre polynomial of degree l has at most $l + 1$ nonzero terms. Although using this fact does not result in a discrete Legendre transform algorithm that is asymptotically faster than the naive algorithm, in practice it does allow for a faster algorithm which is also stable [9] for the band-limits we consider. Of course, at high enough band-limits (say greater than 1023), all algorithms based on a three-term recurrence become unstable (though they are still fast!).

We recognize that other scalar spherical transform algorithms which are asymptotically faster than the semi-naive and naive algorithms exist. However, we still used the semi-naive algorithm in our experiments, basically for two reasons. First, as mentioned already, the semi-naive algorithm, as measured in real time, is faster than the naive algorithm. Second, implementation of the algorithm is simple and straightforward.

There is no reason to believe that using other algorithms would significantly alter our results. We say "significantly" because each algorithm may have its stability quirks. This should be kept in mind when reading our discussion of our results.

To measure the error of the tensor spherical algorithm, we employed the following procedure:

1. Select a band-limit B and rank n.

2. Generate a set of random tensor spherical coefficients f_{lm}^n, uniformly distributed between -1 and 1 for all legal values of l and m, i.e., $0 \le m \le B$, $\max(m, n) \le l \le B$.

3. Synthesize the function

$$\mathbf{v} = \sum_{|n|, |m| \le l \le B} \frac{1}{\|Y_{lm}\|^2} f_{lm}^n \mathbf{Y}_{lm}^n.$$

4. Take the tensor spherical transform of the synthesized function, generating a new set of tensor spherical coefficients h_{lm}^n.

5. Compute the error as

$$\max_{l,m} \left\| f_{lm}^n - h_{lm}^n \right\|.$$

6. Repeat Steps 2–5 ten times.

7. Compute the average absolute and relative errors over the ten trials.

Comments concerning the synthesis done in Step 3 will be made at the end of this section. Also, the random coefficients were chosen so that the resulting function samples would be strictly real. Furthermore, the "extra" Legendre coefficients were calculated using the naive Legendre transform.

In Table I we give the absolute and relative errors for tensor spherical transforms of different ranks at different band-limits.

As can be seen, the error grows worse as the band-limit and rank increase. The source of this poor behavior can easily be identified. Recall that in order to calculate the tensor spherical coefficients, we first compute

$$g^n(l, m) = \left\langle \frac{1}{(\sin \theta)^{|n|}} f, Y_{lm} \right\rangle_{\text{disc}}, \tag{24}$$

where n is the rank of the transform. The subscript "disc" is to remind us that we are now dealing with the discrete inner product. To calculate $g^n(l, m)$, we first divide the sampled signal f by $(\sin \theta)^{|n|}$ and then take the scalar transform of that modified signal.

TABLE I
Tensor Spherical Transforms: Absolute (First Row) and Relative
(Second Row) Errors for Different Bandwidths and Ranks

Band-limit	Rank $= 1$	Rank $= 2$	Rank $= 3$	Rank $= 4$
63	4.2201e-11	1.3648e-10	8.0897e-10	2.2950e-08
	1.6975e-09	2.0537e-09	2.0277e-09	1.0708e-07
127	1.6589e-10	3.6605e-09	1.1327e-07	1.8494e-06
	3.5884e-08	1.4627e-08	2.6641e-07	4.2597e-06
255	5.8974e-10	1.3734e-08	5.6144e-07	2.4696e-05
	3.6359e-08	6.7320e-08	7.2475e-07	1.2126e-04
511	1.1066e-08	9.5600e-07	1.0351e-04	8.2838e-03
	2.2581e-07	3.1972e-06	1.7710e-04	1.6041e-02
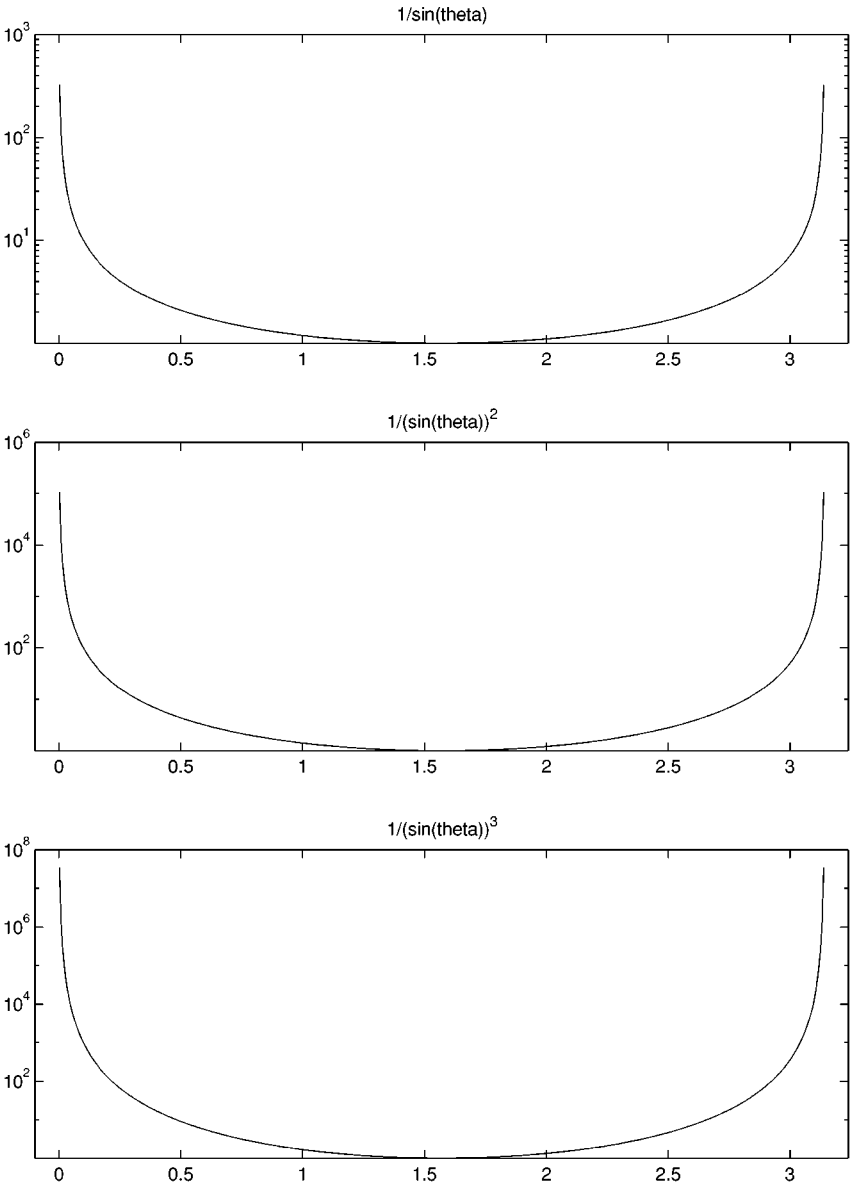
FIG. 3. Semilog plots of $1/(\sin\theta_j)^{|n|}$ for ranks $n = 1, 2,$ and 3 at bandwidth 255.

In Fig. 3 we have plotted $1/(\sin\theta_j)^{|n|}$ for different ranks n at band-limit $= 255$. Dividing the sampled function f by $(\sin\theta_j)^{|n|}$ is "blowing up" those sample values near the ends of the interval. Consequently, accuracy deteriorates as the rank increases, and as the band-limit gets larger, this deterioration simply becomes worse at an even faster rate.

Although the source of the instability cannot be entirely removed, we can easily lessen its influence, at least to some extent. To do so, we must consider the weights used in the Legendre-transform portion of the scalar spherical transform.

By Lemma 4.2, we see that the weights can be written as a product of $\sin\theta$ and a sum involving sines. Therefore, we can "move" one of the sines in $(\sin\theta)^{|n|}$ over to the expression for the weights and hence remove one occurrence of dividing by $\sin\theta_j$. That is, Eq. (24)

now becomes

$$g^n(l, m) = \left\langle \frac{1}{(\sin \theta)^{|n|}} f, Y_{lm} \right\rangle_{\text{disc}}$$

$$= \left\langle \frac{1}{(\sin \theta)^{|n|-1}} f, Y_{lm} \right\rangle_{\text{disc-1}}. \quad (25)$$

The subscript "disc-1" in the above equation means that this discrete inner product is computed using sampling weights a_j (Eq. (23)) which have been divided by $\sin \theta$.

In practice we have found that it is possible to move $\sin^2 \theta$ over to the weights and gain noticeable improvement of accuracy, but that moving larger powers of $\sin \theta$ to the weights does not seem so useful. Hence, the inner product we are evaluating is

$$g^n(l, m) = \left\langle \frac{1}{(\sin \theta)^{|n|}} f, Y_{lm} \right\rangle_{\text{disc}}$$

$$= \left\langle \frac{1}{(\sin \theta)^{|n|-2}} f, Y_{lm} \right\rangle_{\text{disc-2}}. \quad (26)$$

In Fig. 4 we plot the original and modified weights for bandwidth $= 255$. In order to obtain as much accuracy as possible, all modified weights used were computed in Mathematica and then saved to disk. The C code reads in the weights as needed.

Drawing on the point we mentioned at the beginning of this section, this moving of the sines may be necessary because we are using the semi-naive algorithm. That is, there may be some instability issues unique to the semi-naive that we are addressing. Other algorithms may require a slightly different treatment. However, the soundness of our approach to performing tensor spherical transforms, expressing them in terms of scalar spherical transforms, remains.

6.1. *The Errors: A Closer Look*

In Table II we give the absolute and relative errors of the tensor transform algorithm for different band-limits and ranks using the modified weights. Consider the errors at

TABLE II
Tensor Spherical Transforms: Average (First Row) and Relative (Second Row) Errors for Different Band-limits and Ranks Using the Modified (by $\sin^2 \theta$) Weights

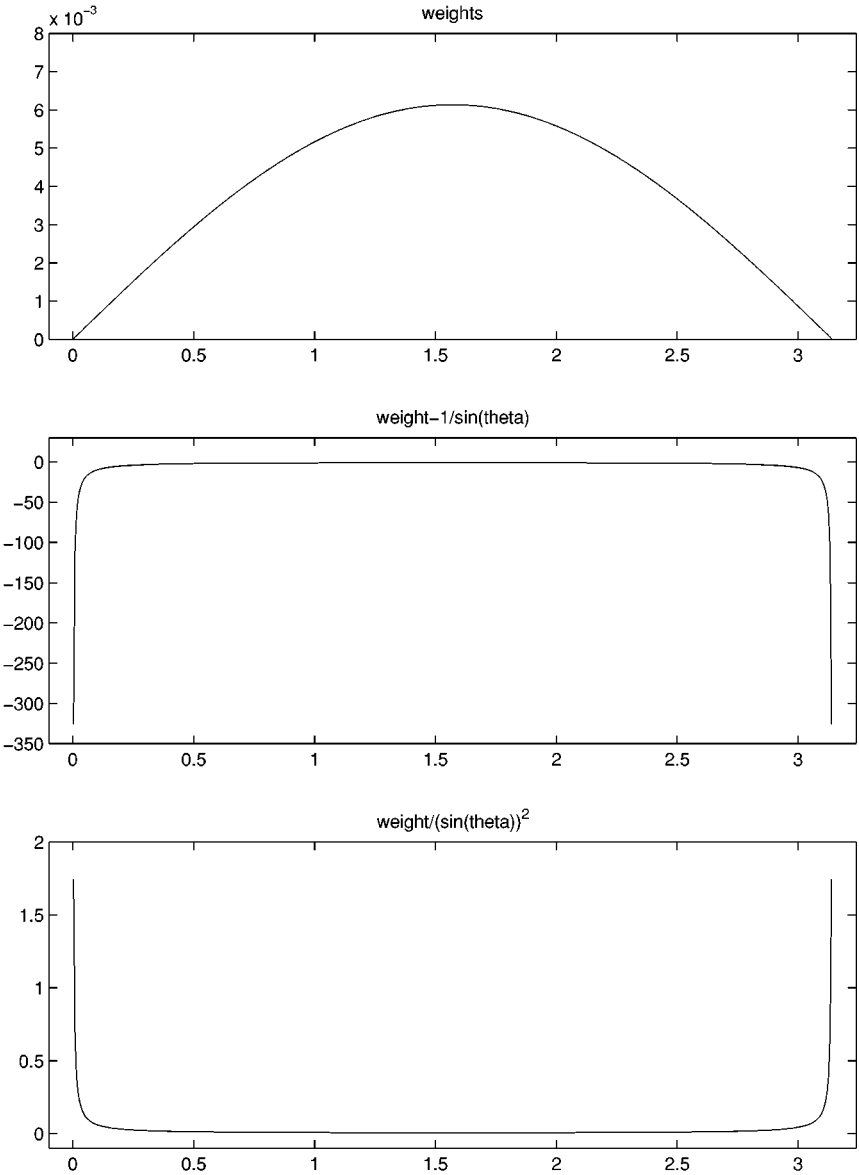| Bandwidth	Rank $= 1$	Rank $= 2$	Rank $= 3$	Rank $= 4$
63	3.3291e-13	2.9555e-12	3.8784e-11	1.1813e-08
	8.5841e-12	1.6776e-11	1.2803e-10	2.1286e-08
127	1.2511e-12	1.3358e-11	3.8273e-10	2.0495e-07
	1.7027e-11	1.1262e-10	2.5266e-09	5.3624e-07
255	5.4060e-12	1.0321e-10	6.0705e-09	6.2496e-06
	3.4873e-10	1.5115e-09	1.3786e-07	1.3923e-05
511	1.5202e-11	1.8197e-09	1.8829e-07	6.5342e-05
	3.8921e-10	5.9895e-09	1.2767e-06	1.6236e-04

FIG. 4.   Original and "modified" weights at band-limit 255.

band-limit $= 255$. For ranks $n = 1, 2, 3$, the errors seem acceptable (at least to us!), for $n = 4$, less so. In order to examine the behavior of the errors more closely, we took the error results of one iteration of the test loop and plotted the maximum absolute and relative errors at *each order m*. That is, given the coefficients computed at order m, calculate the largest absolute and relative error of these coefficients and do this for all orders $0 \leq m \leq 255$. In Figs. 5 and 6 we show semilog plots of the errors for orders $m = 0, \ldots, 50$, for different rank transforms. Note how the errors quickly decay as the order increases. As is obvious in the plots, the largest errors occur at those values of the order m for which m is near the rank n of the transform. The cause of this phenomenon can be identified using the relation between associated Legendre functions and Gegenbauer polynomials.
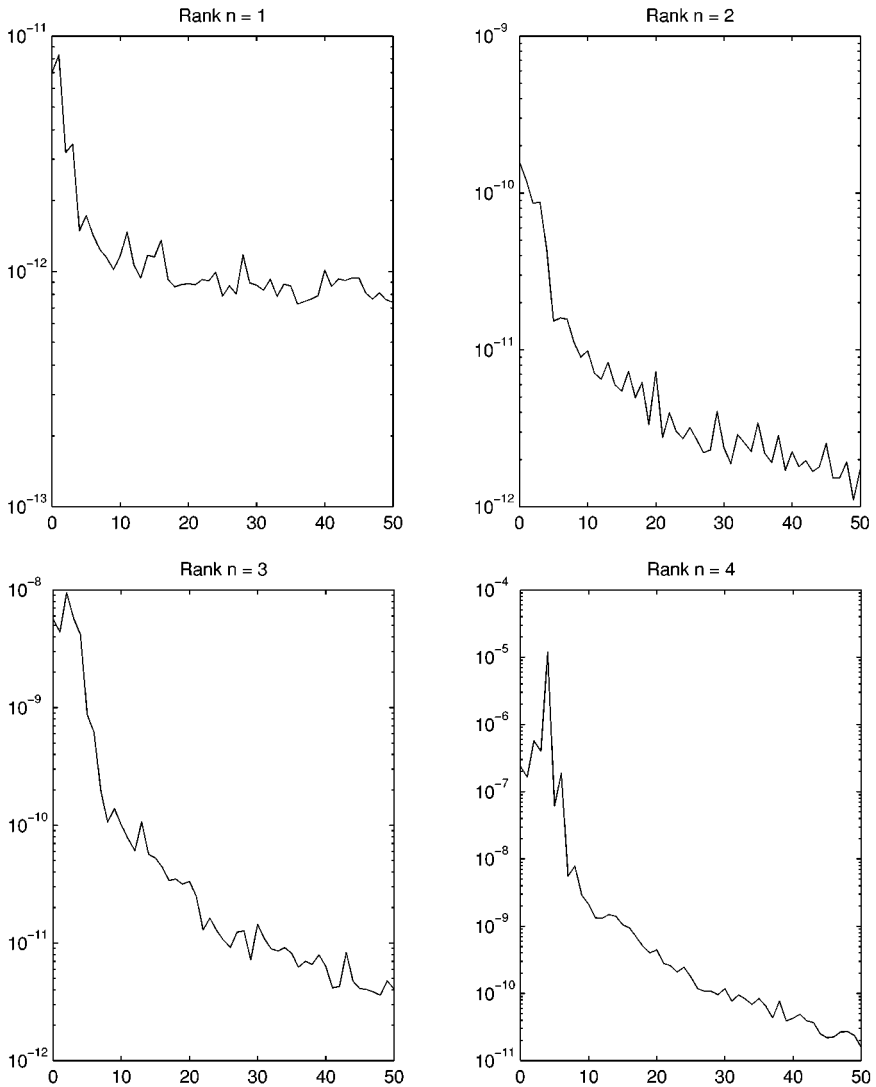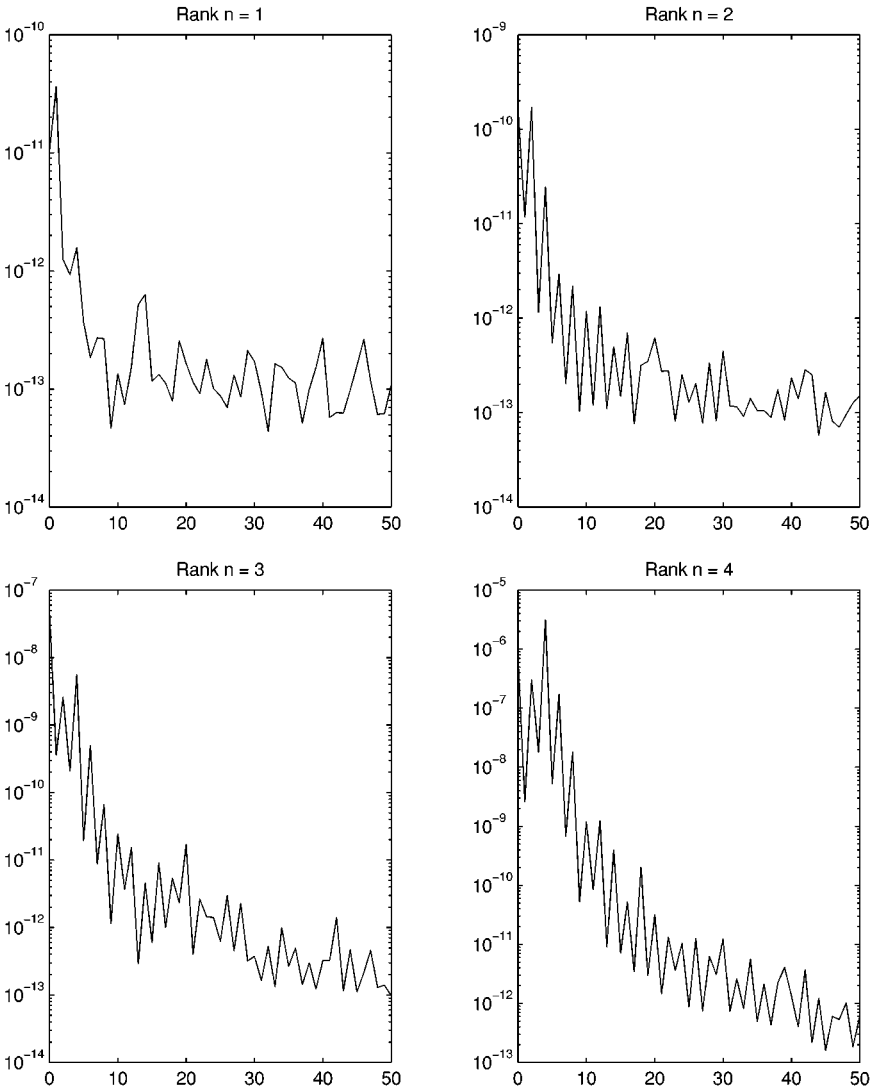
FIG. 5. Band-limit $= 255$, weights modified by $\sin^2 \theta$: Semilog plot of maximum absolute errors of coefficients, for orders $m = 0, \ldots, 50$, for different rank transforms.

Associated Legendre functions may be expressed in terms of Gegenbauer polynomials,

$$P_{lm}(\cos \theta) = A_{lm} \sin^m \theta \times C_{l-m,m+1/2}(\cos \theta),$$

where A_{lm} is a normalizing constant and $C_{lm}(\cos \theta)$ denotes a Gegenbauer polynomial. Note the presence of the $\sin^m \theta$. When the order m is greater than the rank n of the transform, we are effectively no longer dividing by a power of $\sin \theta$. In other words, the higher order associated Legendre functions "absorb" all occurrences of $\sin \theta$. So nowhere is division by small $\sin \theta$ taking place.

Therefore, we conjecture that it is possible to do a still reasonably fast tensor spherical transform, for a reasonable rank at a reasonable band-limit. Extra precision is required only for computing the low order coefficients. The majority of coefficients, for orders m greater than the rank n, could still be computed without special extended (i.e., and possibly slow) precision "handling."

FIG. 6. Bandwidth $= 255$, weights modified by $\sin^2 \theta$: Semilog plot of maximum relative errors of coefficients, for orders $m = 0, \ldots, 50$, for different rank transforms.

6.2. *The Synthesis*

In Step 3 of our procedure for measuring the error of a rank n tensor spherical algorithm, we synthesize the function

$$\mathbf{v} = \sum_{|n|, |m| \leq l \leq B} \frac{1}{\|Y_{lm}\|^2} f_{lm}^n \mathbf{Y}_{lm}^n,$$

where f_{lm}^n were randomly generated tensor spherical coefficients. By the definition of $\mathbf{Y}_{lm}^n$ (Corollary 3.1), this involves dividing a sampled scalar spherical harmonic Y_{lm} by $(\sin \theta)^{|n|}$. From the results we have presented, we know that the principle source of error in evaluating the inner products is the division by $(\sin \theta)^{|n|}$. By moving $\sin^2 \theta$ over to the weights, the error is somewhat (though not greatly) reduced.

However, since division by $(\sin\theta)^{|n|}$ is part of the synthesis step, a legitimate question to ask is how much error is present in the sampled function **v** itself, before any spherical transforms are computed. Reporting error values obtained from the use of dubious sampling data would not be of much value. We want to test the tensor algorithm and *not* the sampling + tensor algorithm. To accomplish this, we used Mathematica.

As a means of testing the tensor algorithm alone, we ran the following experiment. For band-limit $B = 255$ and rank $n = 4$, we set the tensor coefficients as follows:

$$f_{lm}^n = \begin{cases} 1 & \text{if } m \geq 0 \\ 0 & \text{otherwise} \end{cases} \tag{27}$$

Next, we sampled **v** in Mathematica. This sampling can be done at high precision and we can control this precision too. The sample values generated were then written to disk and it was this data that was read into the C code and tensor-transformed. The differences between the errors obtained using the Mathematica data as input data and the errors produced using the C-generated input data were minimal. Therefore, the errors we are seeing are not entirely due to the sampling. Those errors really do result when the tensor transform algorithm is implemented in a finite-precision fashion.

7. CONCLUSION

We have described algorithms for the numerical computation of Fourier transforms of tensor fields on the two-sphere, S^2. These algorithms reduce the computation of an expansion on tensor spherical harmonics to expansions in scalar spherical harmonics and hence can take advantage of improvements in the computation of scalar spherical harmonic transforms.

Although the algorithms we describe are susceptible to certain numerical instabilities, we present numerical results which indicate that minor variations of the algorithms can produce stable results for a useful range of bandwidths and ranks.

REFERENCES

1. B. Alpert and V. Rokhlin, A fast algorithm for the evaluation of Legendre transforms, *SIAM J. Sci. Statist. Comput.* **12**, 158 (1991).

2. G. A. Dilts, Computation of spherical harmonic expansion coefficients via FFT's, *J. Comput. Phys.* **57**, 439 (1985).

3. J. R. Driscoll and D. Healy, Computing Fourier transforms and convolutions on the 2-sphere, *Proc. 34th IEEE FOCS* (1989), pp. 344–349 (extended abstract); *Adv. in Appl. Math.* **15**, 202 (1994).

4. J. R. Driscoll, D. Healy, and D. Rockmore, Fast discrete polynomial transforms with applications to data analysis for distance transitive graphs, *SIAM J. Comput.* **26**, 1066 (1997).

5. C. A. J. Fletcher, *Computational Techniques for Fluid Dynamics* (Springer-Verlag, New York, 1988).

6. F. A. Gilbert, Inverse problems for the earth's normal modes, in *Mathematical Problems in the Geophysical Sciences*, Vol I (American Mathematical Society, Providence, RI, 1971).

7. I. Gel'fand, R. Minlos, and Z. Shapiro, *Representations of the Rotation and Lorentz Groups and Their Applications* (MacMillan, New York, 1963).

8. J. Goldberg, A. Macfarlane, E. Newman, F. Rohrlich, and E. Sudarshan, Spin-*s* spherical harmonics and $\eth$, *J. Math. Phys.* **8**, 2155 (1967).

9. D. Healy, D. Rockmore, P. Kostelec, and S. Moore, FFTs for the 2-Sphere—Improvements and Variations, *Adv. in Appl. Math.*, to appear.

10. D. Maslen, *Sampling of Functions and Sections for Compact Groups*, Technical Report PMA-TR99-193 (Department of Mathematics, Dartmouth College, Hanover, NH, October, 1999).

11. D. Maslen, *Fast Transforms and Sampling for Compact Groups*, Ph.D. thesis (Department of Mathematics, Harvard University, 1993).

12. M. J. Mohlenkamp, Fast transforms for spherical harmonics, *J. Fourier Anal. Appl.* **5**, 159 (1999).

13. P. Morse and H. Feshbach, *Methods of Theoretical Physics* (McGraw-Hill, New York, 1953).

14. E. Newman and R. Penrose, Note on the Bondi-Metzner-Sachs group, *J. Math. Phys.* **7**, 836 (1966).

15. S. Orzag, Fast eigenfunction transforms, in *Science and Computers* (Academic Press, Orlando, 1986).

16. D. Potts, G. Steidl, and M. Tasche, Fast and stable algorithms for discrete spherical Fourier transforms, *Linear Algebra Appl.* **275–276**, 433 (1998).

17. SpharmonicKit is a freely available collection of C programs for doing Legendre and scalar spherical transforms. Developed at Dartmouth College by S. Moore, D. Healy, D. Rockmore, and P. Kostelec, it is available at www.cs.dartmouth.edu/~geelong/sphere.

18. P. Swarztrauber, The vector harmonic transform method for solving partial differential equations in spherical geometry, *Mon. Weather Rev.* **121**, 3415 (1993).

19. C. Temperton, On scalar and vector transform methods for global spectral models, *Mon. Weather Rev.* **119**, 1303 (1991).

20. T. Wu and C. Yang, Dirac monopole without strings: Monopole harmonics, *Nucl. Phys. B* **107**, 365 (1976).

21. T. Wu and C. Yang, Some properties of monopole harmonics, *Phys. Rev. D* **16**, 1018 (1977).

22. M. Zaldarriaga and U. Seljak, An all-sky analysis of polarization in the microwave background, *Phys. Rev. D* **55**, 1830 (1997).